International Journal of Advanced Technology in Engineering and Science
Vol. No.5, Issue No. 03, March 2017
www.ijates.com
ijates
ISSN 2348 - 7550

# A STUDY OF MECHANISM OF AN APERTURE-COUPLED DUAL STACKED MICROSTRIP PATCH ANTENNA FED BY COPLANAR WAVEGUIDE

**Thirandasu.Swathi[1], M.Praveena Reddy [2], Razia Mohammadi [3]**

[1,2,3]*Assistant Professor, Ece Dept, Sphoorthy Engineering College*
*Telangana, Hyderabad (India)*

## ABSTRACT

*An aperture-coupled stacked patch antennas, fed by coplanar waveguide (CPW) is presented which is to be used at millimetre-wave frequencies. After studying the important design parameters, it was found that impedance matching can easily be achieved by tuning the dimensions of the excitation slot and adding an impedance tuning stub. In this way, an antenna element with a –10 dB impedance bandwidth of over 35 % was designed. This study allows a more efficient design of CPW-fed stacked patch antennas which has led for coupling mechanism between the different resonators.*

## I. INTRODUCTION

To feed antennas operating at millimeter-wave frequencies (around 30 GHz), Aperture coupling is an interesting technique. Micro strip antennas become very small, reducing the suitability of coaxial feeding, as probes are accompanied by soldering points, introducing parasitic inductances at these frequencies. However, Aperture coupling provides lower parasitic radiation and the centred feed provides higher radiation pattern symmetry [3]. The dimension variation of the aperture facilitates impedance matching [3]. It is known that the coupling of several resonances leads to a significant increase in bandwidth, which is desired in many applications in the field of telecommunications, e.g. for wireless links with high information capacity. In this paper a systematic parameter study of an aperture-coupled stacked dual patch antenna on glass substrates with an intermediate permittivity ($\varepsilon_r$ = 6.2), fed by CPW is focused and thus eliminating the need for a separate feed substrate, which was required to accommodate the feeding microstrip line in [2]. Recently CPW has several advantages: low dispersion, good characteristic impedance control, easy integration with shunt lumped elements and active devices [1].

CONFIGURATION OF AN ANTENNA

In below Fig. 1, the antenna configuration consists of a ground plane carrying the CPW terminated in an excitation slot, a substrate, a lower square patch, a second substrate on top of it and an upper square patch. The slot is short-circuited by connecting the centre conductor of the CPW to the ground plane. The slot is inductively coupled because the impedance locus lies in the inductive region on the Smith chart. This configuration allows easier impedance matching than its counterpart, the capacitively coupled slot, which is open-circuited [4]. Therefore the inductively coupled excitation slot is chosen for an investigation of the stacked patch

configuration.

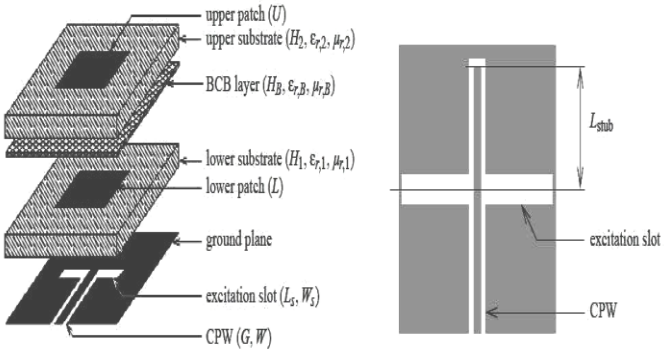


Fig. 1: Stacked patch antenna configuration (left) and impedance tuning stub layout (right)

The lower substrate has thickness $H_1$, relative permittivity $\varepsilon_{r;1}$ and relative permeability $\mu_{r;1}$. The upper substrate has thickness $H_2$, relative permittivity $\varepsilon_{r;2}$ and relative permeability $\mu_{r;2}$. A Multi Chip Module technology with deposited thin films (MCM-D) is used to build some test antennas. This technology focuses on glass substrates ($\varepsilon_{r;1} = \varepsilon_{r;2} = 6.2$ and $\mu_{r;1} = \mu_{r;2} = 1$) for their ease of treatment during the process and for the low material cost. The main interest here was to construct a high bandwidth antenna using these glass substrates, despite the relatively high permittivity. Both substrates are glued together by a thin BenzoCycloButene (BCB) film (with parameters $H_B = 5$ µm, $\varepsilon_{r;B} = 2.7$, $\mu_{r;B} = 1$). Because the BCB layer's thickness is very small compared to the considered wavelengths, its influence is negligible. The excitation slot has length *Ls* and width *Ws*. The patches are centred with respect to each other and the excitation slot is aligned under the centre of the patches. The coplanar waveguide has a centre conductor width *W* and a slot width *G*.

STUDY OF VARIOUS PARAMETERS

Here a systematic parameter study is performed. The dimensions of the CPW are chosen such that an odd mode characteristic impedance of 50 Ω is obtained: $G = 25$ µm and $W = 100$ µm. Resonant frequencies are defined at maxima of the real part of the input

impedance *Z*in( *f* ). The two patches and the excitation slot in the ground plane form a resonating structure, which exhibits two coupling effects: one between the slot and the lower patch, another between the patches. The self-resonance of the excitation slot lies above the considered frequency band (20–45 GHz). On the Smith chart the impedance locus contains two loops. The larger the radius of such a loop, the greater the coupling factor. Each physical parameter, except for $\varepsilon_{r;1}$ and $\varepsilon_{r;2}$, will be varied, keeping the other parameters fixed, and its influence will be discussed. Unless mentioned otherwise, the slot width *Ws* = 0:1 mm and the stub length *L*stub = 0.8 mm. The analysis is based on the solution of integral equations solved in the spectral domain by the method of moments. Agilent Technologies' Momentum is used as a simulation tool. For this structure, a mesh of 20 cells per wavelength, combined with edge expansion functions, gives accurate results. The electric and magnetic surface currents are discretized using rooftop expansion functions defined over the cells in the mesh.

By Varying the Excitation Slot Dimensions *Ls* and *Ws*

The length *Ls* of the excitation slot is another parameter which has a considerable influence on the resonant frequencies and on the impedance behaviour. It is observed that *f*1 shifts down and *R*1 rises as *Ls* is increased. If *X*1 = Im*f*Z*in*( *f*1)g, it is observed that *X*1 _ *Ls*, which is a result similar to those in [2], [4] and [6]. Frequency *f*2

shifts down for increasing *Ls*, but this shift is quite small compared to that of *f*1. This seems logical since *f*2 is mainly determined by *U* and the upper patch is somewhat shielded from the excitation slot by the lower patch. On the Smith charts in Fig. 2 the main loop becomes larger for increasing *Ls*. For a certain value of *Ls*, this loop will touch the circle *r* = 1. Therefore, this parameter can be used for impedance matching, if the inductive component *X*1 can be neutralized. The radius of the small loop increases as *Ls* is increased, reaches a maximum and decreases again for very large *Ls*. This smaller loop rotates in a clockwise direction with respect to the main loop as *Ls* increases.

The parameter *Ws* has an effect similar to that of *Ls*. It is observed that *f*1 decreases slightly and *R*1 as well as *X*1 increase almost linearly with increasing *Ws*.

By Varying the Substrate Thicknesses $H_1$ and $H_2$

The first resonance ($f_1$, $R_1$) is affected by the thickness *H*1 of the lower substrate. The *f*1 shifts down as *H*1 is increased. The influence of *H*1 on the second resonance is small. It is noted that the bandwidth of the first resonance increases as *H*1 is increased. On the Smith chart the radius of the lower frequency loop decreases if *H*1 is increased. This behaviour was expected as the patch is moved further away from the excitation slot, thus reducing the coupling [5].

The thickness *H*2 of the upper substrate has a considerable influence on both resonances and on the input impedance. An important consequence of raising *H*2 is an increase in bandwidth. Another observation is that *f*2 shifts down more than *f*1 if *H*2 is increased, so the ratio *f*2= *f*1 is lowered and the two resonant frequencies lie closer to each other, which is also noted in. The impedance curve versus frequency becomes smoother. On the Smith charts in Fig. 3, the radius of the smaller loop in the impedance locus and the coupling between the two patches decrease as $H_2$ is raised.

Design Process

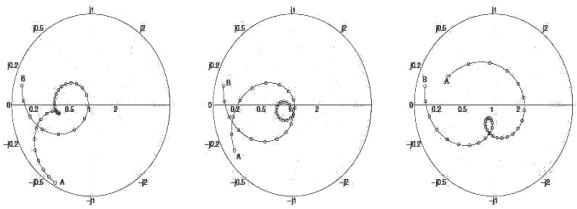

Fig.2 : Impedance loci: (a) $L_s = 1.4$ mm, (b) $L_s = 1.7$ mm and (c) $L_s = 2.0$ mm. Other parameters: $H_1 = 0.3$ mm, $H_2 = 0.7$ mm, $L = 1.4$ mm, $U = 1.4$ mm. Frequency range A-B: 21-38 GHz with 0.5 GHz increments.

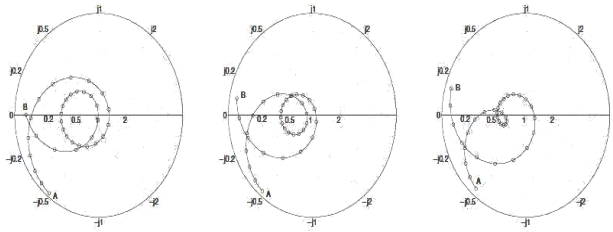

Fig.3 : Impedance loci: (a) $H_2 = 0.5$ mm, (b) $H_2 = 0.6$ mm and (c) $H_2 = 0.7$ mm. Other parameters: $H_1 = 0.3$ mm, $L = 1.4$ mm, $U = 1.45$ mm, $L_s = 1.55$ mm. Frequency range A-B: 21-38 GHz with 0.5 GHz increments.

A tuning stub was added to achieve impedance matching as shown in Fig. 1 for the design of a wide-band test antenna around 30 GHz. The required stub length $L_{stub}$ is shorter for an electrically open-ended stub than for an electrically short-circuited stub and is approximately □$_1$/4, where $\lambda_1 = \lambda_0 / \sqrt{\varepsilon_1}$ and □$_0$ is the free space wavelength [7][8]. This antenna's physical parameters are: $H_1$ =0.3 mm, $H_2$ =0.7 mm, *L* =1.4 mm, *U* =1.425

mm, $L_s$ =1.58 mm, $W_s$ =0.1 mm. Its main characteristics are: $f_1$ = 25.2 GHz, $f_2$ = 33.2 GHz, $R_1 = R_2 \approx 60$ □ . The –10 dB bandwidth is 10.73 GHz or 36.8 %, while the –15 dB bandwidth is still 9.27 GHz or 31.8 % [9]. The antenna gain in broadside direction is about 3 dB and shows two maxima, which are each located higher in frequency than the input resistance maxima at $f_1$ and $f_2$.

## II. CONCLUSIONS

For better understanding of the mechanism of an aperture-coupled dual stacked patch configuration fed by coplanar waveguide, more simulations have been done. The summarized results in this paper are of practical importance to designers of this type of antenna element. Careful inspection of the results of this study has allowed to design a wide-band antenna with a –10 dB bandwidth of over 35 %. It is especially for the glass substrates employed in MCM-D technology, but the main trends in the results can surely be extended to substrates with different permittivity's.

## REFERENCES

[4] Mohammad Tehranipoor, Mehrdad Nourani, Nisar Ahmed, "Low Transition LFSR for BIST Based Applications"

[5] S.C. Lei, X.Y.Hou ,Z.B.Shao and F.Liang," A class of SIC circuits: theory and application in BIST design," IEEE trans. circuits syst. II, vol.55,no.2,pp.161-165,Feb.2008.

[6]. DS-LFSR : A BIST TPG for Low Switching Activity. Seongmoon Wang, Sandeep K. Gupta. IEEE transactions on Computer-Aided Design of Integrated Circuits and Systems. Vol.21,No 7 July 2002.

[7].Low Power Testing of VLSI Circuits: Problems and Solutions by Patrick Gigard, member, IEEE.

[8]. N. Ahmed, M. Tehranipoor, and M. Nourani, "Low Power Pattern Generation for BIST Architecture," Proc. Int'l Symp. Circuits and Systems, vol. 2, pp. 689-692, 2004.

[9]. M. Tehranipoor, M. Nourani, and N. Ahmed, "Low Transition LFSR for BIST-Based Applications," Proc. IEEE 14th Asian Test Symp, 2005.

[10]. F.Corno, M.Rebaudengo, M.Sonza Reorda, "A Test Pattern Generation Methodology for Low Power Consumption", pp.1-5, 2008.

[11]. Tiwari, Honey Durga, et al., "Multiplier design based on ancient Indian Vedic Mathematics," Int. SoC Design Conf., 2008, vol. 2. IEEE Proc., pp. II-65 - II-68.

[12]. N. Basturkmen, S. Reddy, and I. Pomeranz, "A Low Power Pseudo-Random BIST Technique," Proc. 1st International Conference on Computer Design, pp. 468- 473, 2002.

[13]. X. Zhang and K. Roy, "Peak Power Reduction in Low Power BIST," in Proc. Int. Symp. on Quality Elect. Design (ISQED'01), pp. 425-432, 2001.

[14].P.Girard, L.Guiller, C.Landrault, Pravossoudovitch,and H.J.Wunderlich, " A modified clock scheme for a low power BIST test pattern generator," 19th IEEE proc. VLSI test Symp.,CA,pp-306- 311,Apr-May 2001.